Electronic Supplementary Material (ESI) for RSC Advances.

Supplementary Data

Beyond the Pristine MOFs: Carbon Dioxide Capture by Metal-Organic Frameworks (MOFs)-Derived Porous Carbon Materials

Hye Ryeon Kim,[a] Tae-Ung Yoon,[c] Seung-Ik Kim,[c] Jihyun An*[b], Youn-Sang Bae*[c], and Chang Yeon Lee*[a],[d]

[a]Department of Energy and Chemical Engineering, Incheon National University, 119, Academy-ro, Yeonsu-gu, Incheon, 22012, Republic of Korea

[b]Department of Chemistry Education, Seoul National University, 1 Gwanak-ro, Gwanak-gu, Seoul, 08826, Republic of Korea.

[c]Department of Chemical and Biomolecular Engineering, Yonsei University, 50 Yonsei-ro, Seodaemun-gu, Seoul, 03722, Republic of Korea

[d]Innovation Center for Chemical Engineering, Incheon National University, 119, Academy-ro, Yeonsu-gu, Incheon, 22012, Republic of Korea

S1. Experimental Section

Materials

Zinc nitrate hexahydrate, zinc acetate dihydrate, terephthalic acid, 4,4'-biphenyldicarboxylic acid, adenine, methanol and chlorobenzene were purchased from Aldrich Chemical. N,N-diethylformamide (DEF) was purchased from TCI. N,N-dimethylformamide (DMF) was purchased from Fisher Scientific. 4,4',4''-benzene-1,3,5-triyl-tribenzoic acid (H_3BTB) was synthesized according to the synthesis procedure reported in literature.

Preparations of porous carbon materials

MOF-5, MOF-177 and bioMOF-100 samples were synthesized following the synthesis procedures reported in literatures. In order to obtain porous carbon materials, MOF-5, MOF-177 and bio-MOF-100 were placed in a quartz tube furnace and carbonized. The carbonization was performed at 1000 °C for 6 hours with a heating rate of 5 °C/min under an Ar flow. The resulting carbon materials were denoted as M5-1000, M177-1000 and B100-1000, respectively.

Characterizations

Powder X-Ray diffraction (XRD) data were collected on a Rigaku smartlab diffractometer using Cu Kα radiation (λ = 1.5412 Å). The morphologies before and after carbonization process were characterized by using scanning electron microscopy (SEM) on a JEOL JSM-7800F microscope. Raman spectra were obtained on a WITEC alpha300 spectrometer using a helium neon laser (532 nm). X-ray photoelectron spectroscopy (XPS) measurements were performed on a PHI 5000 VersaProbe ll X-ray photoelectron spectrometer. Porosity characteristics of the samples were characterized by measuring nitrogen adsorption isotherms at 77K using an adsorption analyzer (Autosorb-iQ, Quantachrome Instruments). Prior to adsorption measurements, the carbonized samples were evacuated at 150°C for 5 hours under vacuum. The specific surface areas were calculated using Brunauer–Emmett–Teller (BET) method in the linear range (M5-1000; $0.0100 < P/P_0 < 0.0994$, M177-1000; $0.0100 < P/P_0 < 0.0993$, B100-1000; $0.0070 < P/P_0 < 0.0395$). CO_2 adsorption isotherms were obtained using an adsorption analyzer

(Autosorb-iQ, Quantachrome Instruments). Prior to adsorption measurements, the samples were activated at 150 °C for 5 hours using an outgas port of the Autosorb-iQ instrument.

IAST calculations

In order to predict adsorptive behaviors of a two-component gas mixture from single-component isotherms, we used the Ideal Adsorbed Solution Theory (IAST) of Myers and Prausnitz. The IAST adsorption selectivity for CO_2/N_2 (15% CO_2, 85% N_2) and CO_2/CH_4 (50% CO_2, 50% CH_4) at 298 K were calculated. The adsorption selectivity for the two-component mixture is defined by $S=(q_1/p_1)/(q_2/p_2)$.

Breakthrough experiments

The breakthrough experiments were carried out in a custom-built system illustrated in Fig. S1. Five mass flow controllers (0~100 mL/min) (Bronkhorst, Germany) were used to regulate the gas flow rates. By combining two N_2 streams and two CO_2 streams with a humidifier, dry and humid CO_2/N_2 mixtures were generated. The column was placed in a ventilated thermostatted oven for measurements at a constant temperature. The gas composition at the outlet of the column was measured online by a mass spectrometer (Pfeiffer Vacuum Prisma QME 200, Germany).

To avoid large pressure drops, the powder sample was pelletized using a carver press (Carver, Inc., USA). The obtained pellets with a size of 500~1000 μm were initially activated at 423 K for 5 hours under vacuum. The activated pellets (153 mg) were then packed into a stainless steel column with a length of 15 cm and an internal diameter of 0.44 cm. The remainder of the column was filled with glass beads with a diameter of 750 μm. The column was then degassed by a He flow of 40 mL/min at 423 K for 1 hour to remove all the impurities adsorbed during the packing procedure. Between each measurement, a He flow of 40 mL/min at 303 K was introduced into the column for at least 10 min.

At t=0, the He flow was switched to a flow of dry or humid CO_2/N_2 mixture (CO_2:N_2 = 15:85, total flow rate = 40 mL/min).

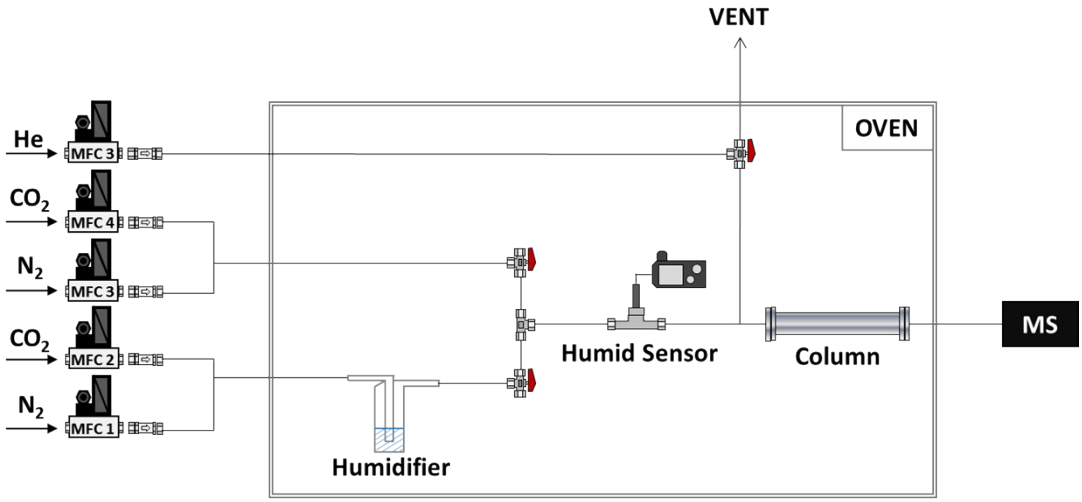

Figure S1. A schematic diagram of the dynamic breakthrough experimental setup. MS: Mass spectrometer, MFC: Mass flow controller, P: Pressure transducer.

S2. Powder X-ray diffraction (PXRD) patterns

(a)

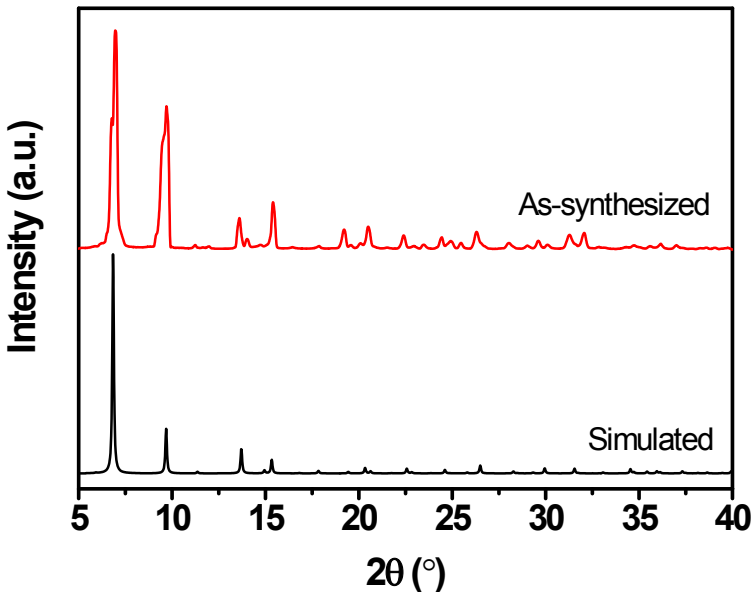

(b)

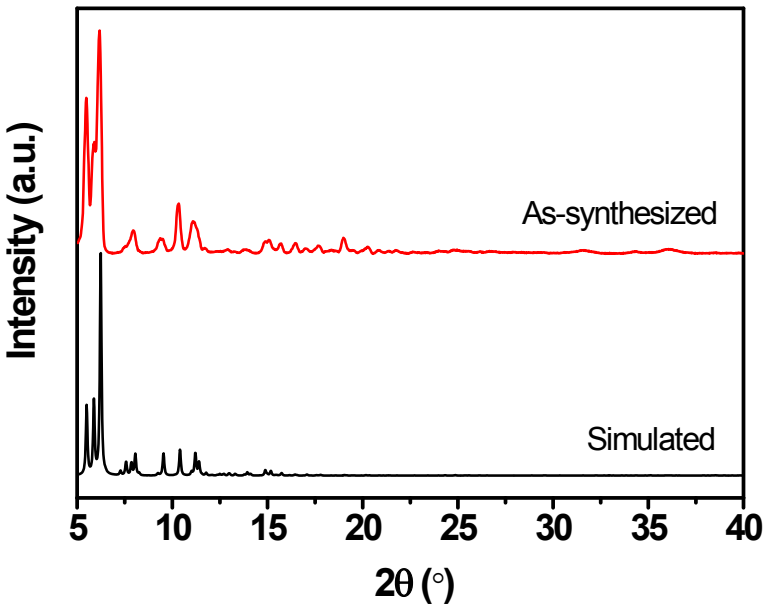

(c)

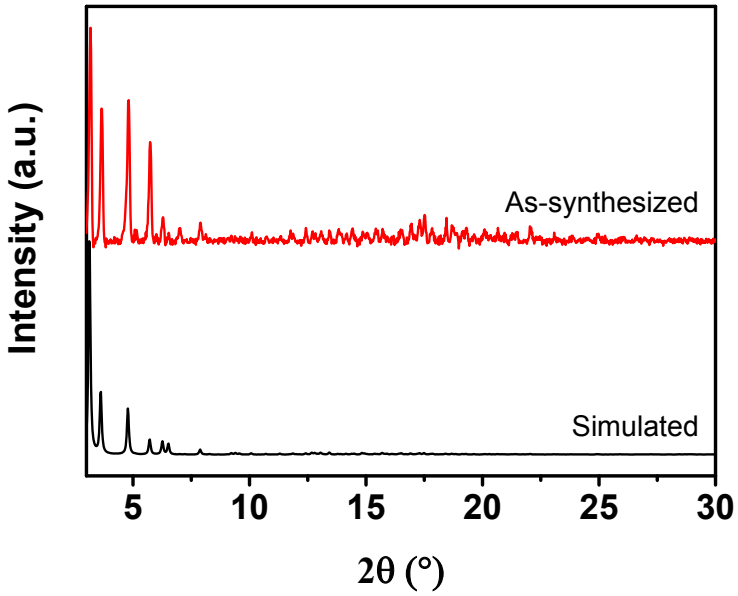

Figure S2. PXRD patterns of (a) MOF-5, (b) MOF-177, (c) bioMOF-100.

S3. Scanning electron microscopy (SEM)

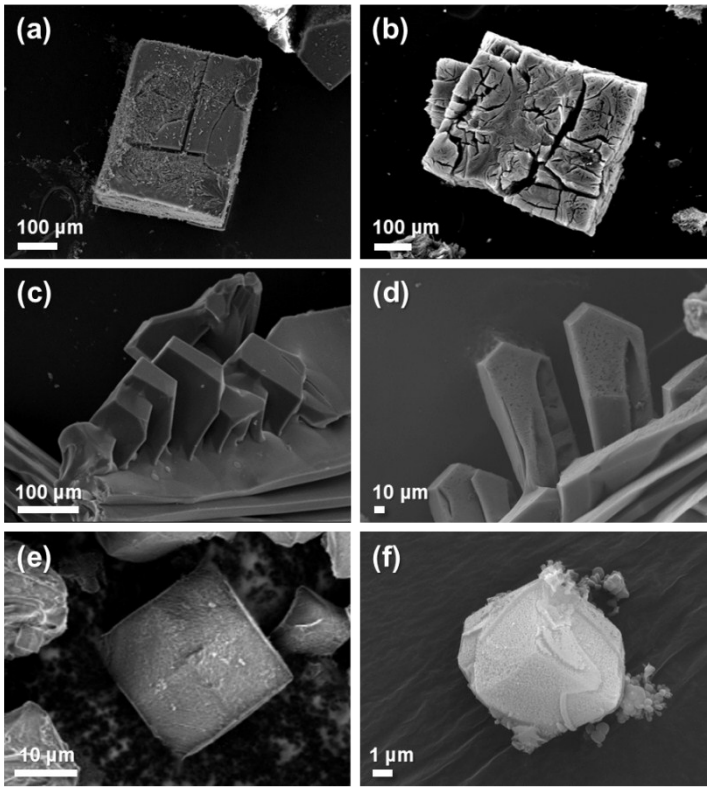

Figure S3. SEM images of (a) MOF-5, (b) M5-1000, (c) MOF-177, (d) M177-1000, (e) bioMOF-100 and (f) B100-1000.

(a)

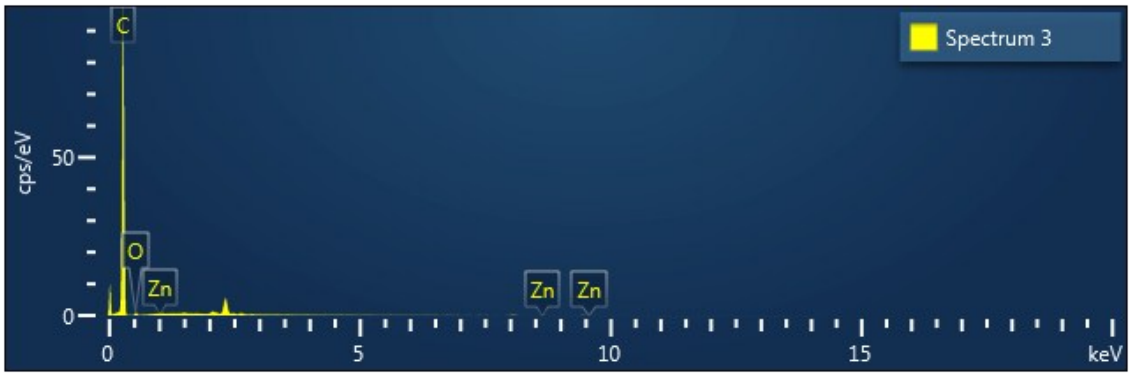

(b)

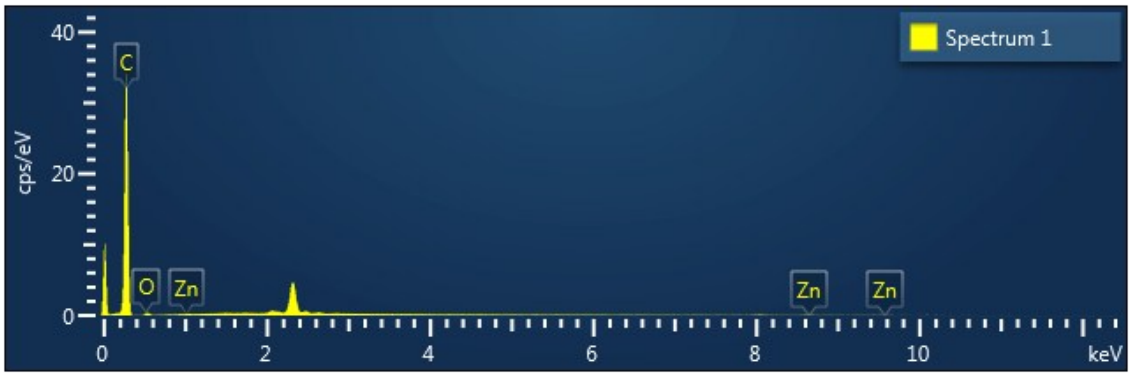

(c)

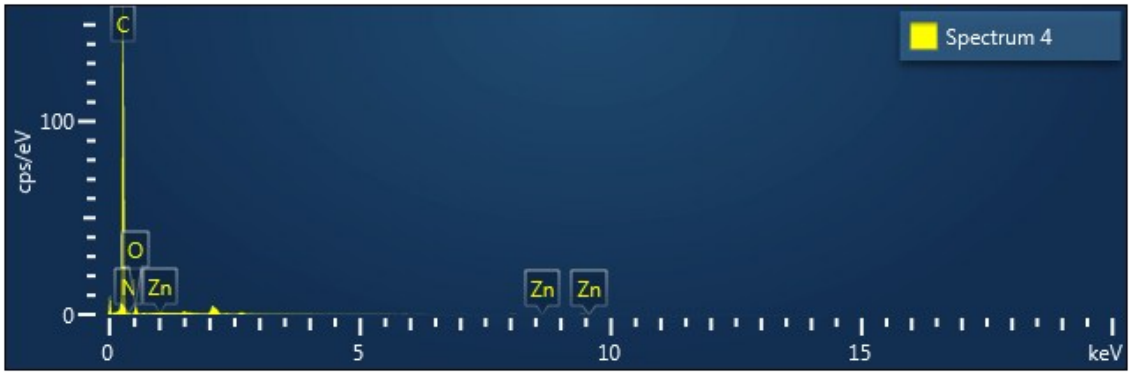

Figure S4. SEM-EDS spectra of (a) M5-1000, (b) M177-1000, (c) B100-1000.

S4. X-ray photoelectron spectroscopy (XPS) spectra

(a)

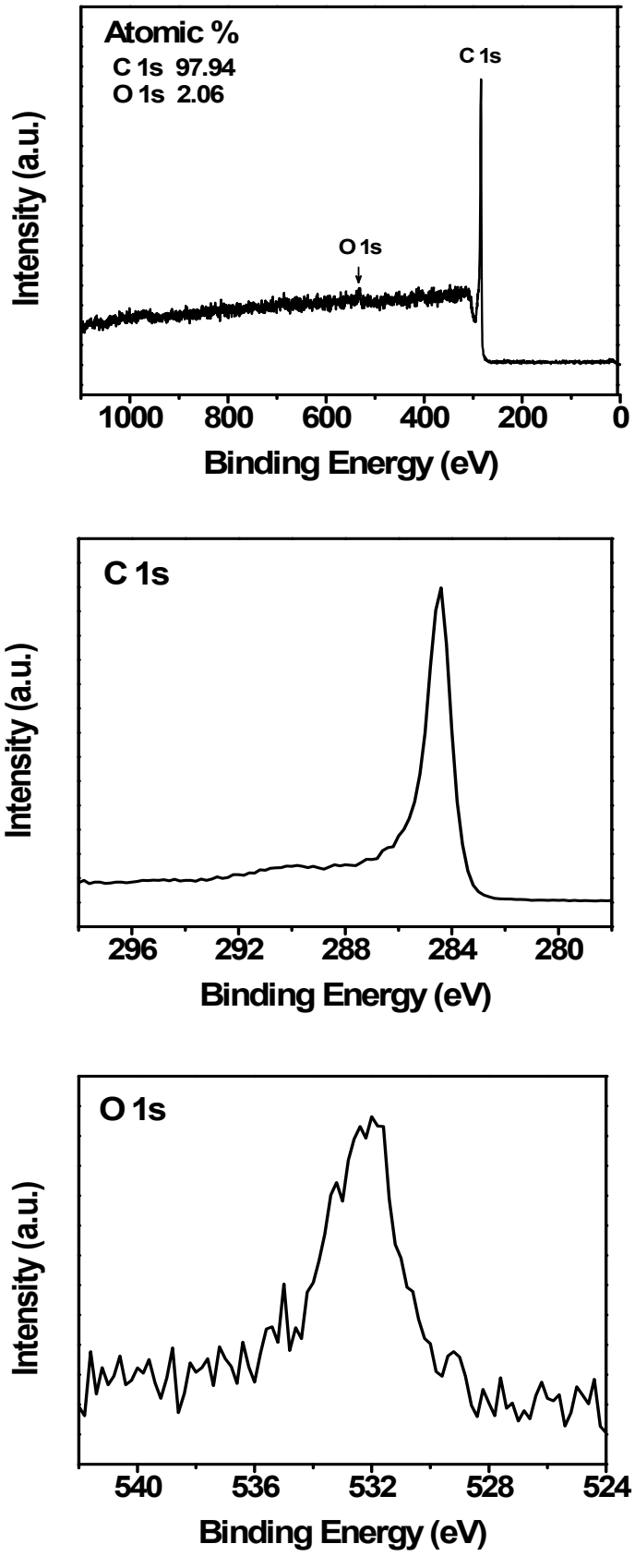

(b)

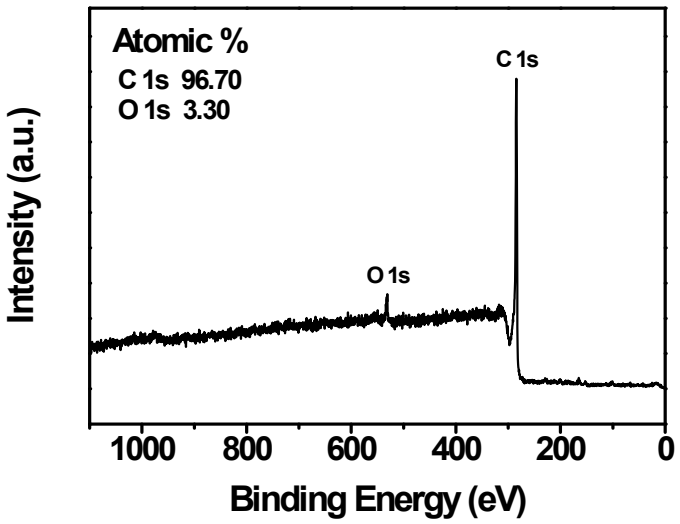
Atomic %
C 1s 96.70
O 1s 3.30
C 1s
O 1s
Intensity (a.u.)
1000
800
600
400
200
0
Binding Energy (eV)

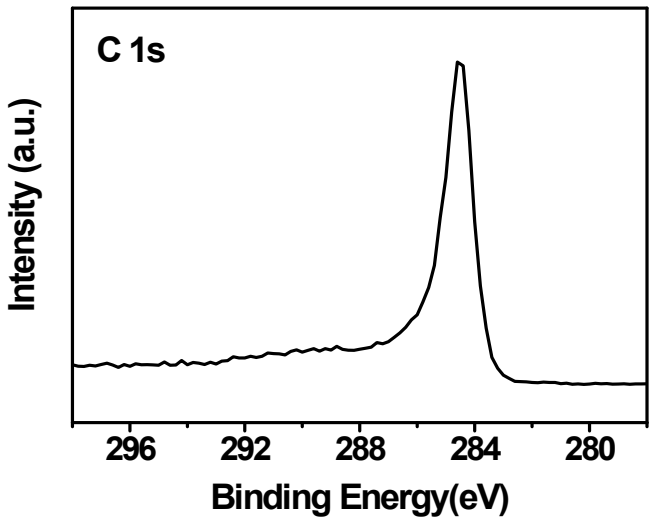
C 1s
Intensity (a.u.)
296
292
288
284
280
Binding Energy(eV)

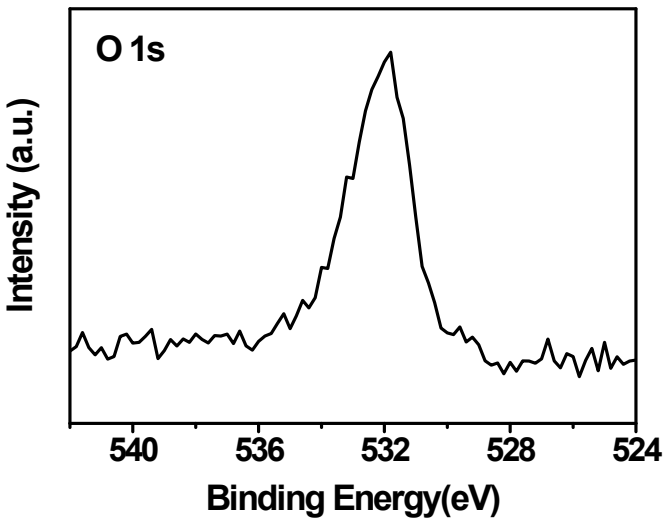
O 1s
Intensity (a.u.)
540
536
532
528
524
Binding Energy(eV)

(c)

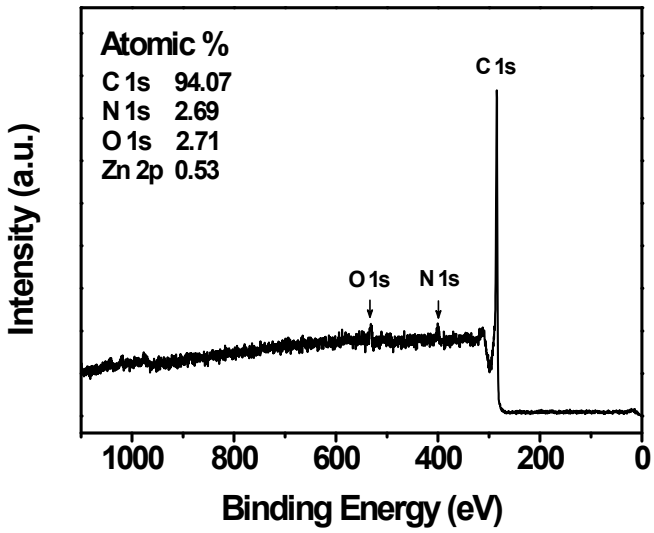
Atomic %
C 1s 94.07
N 1s 2.69
O 1s 2.71
Zn 2p 0.53
C 1s
O 1s
N 1s
Intensity (a.u.)
1000
800
600
400
200
0
Binding Energy (eV)

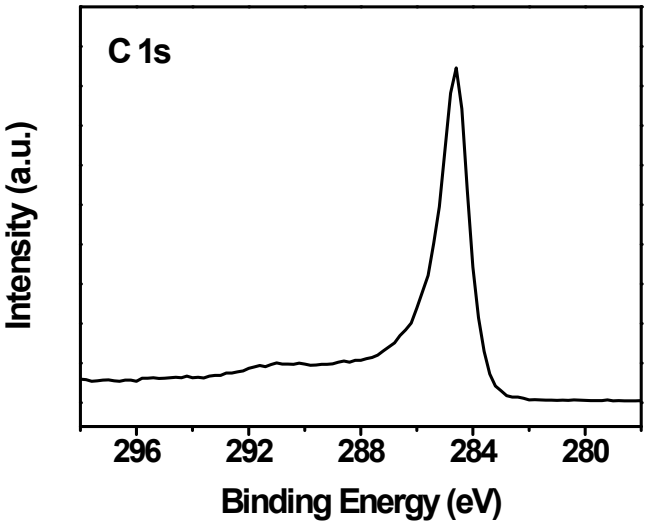
C 1s
Intensity (a.u.)
296
292
288
284
280
Binding Energy (eV)

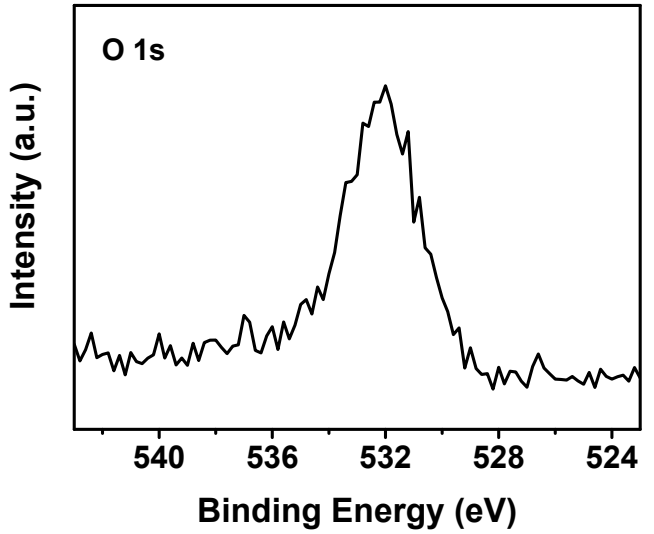
O 1s
Intensity (a.u.)
540
536
532
528
524
Binding Energy (eV)

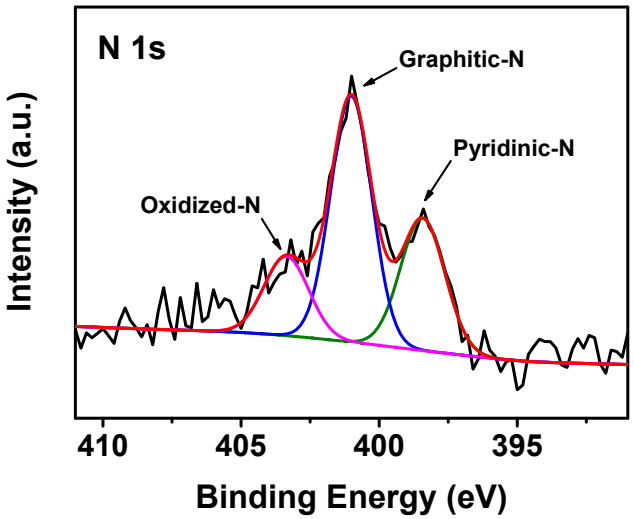

Figure S5. XPS spectra of (a) M5-1000, (b) M177-1000 and (c) B100-1000.

S5. BET plots

(a)

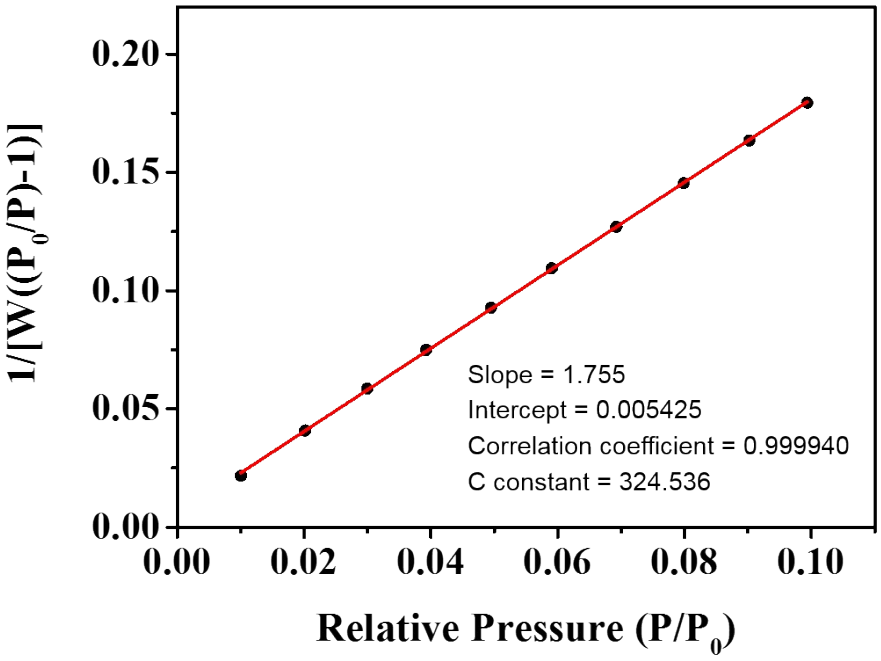

(b)

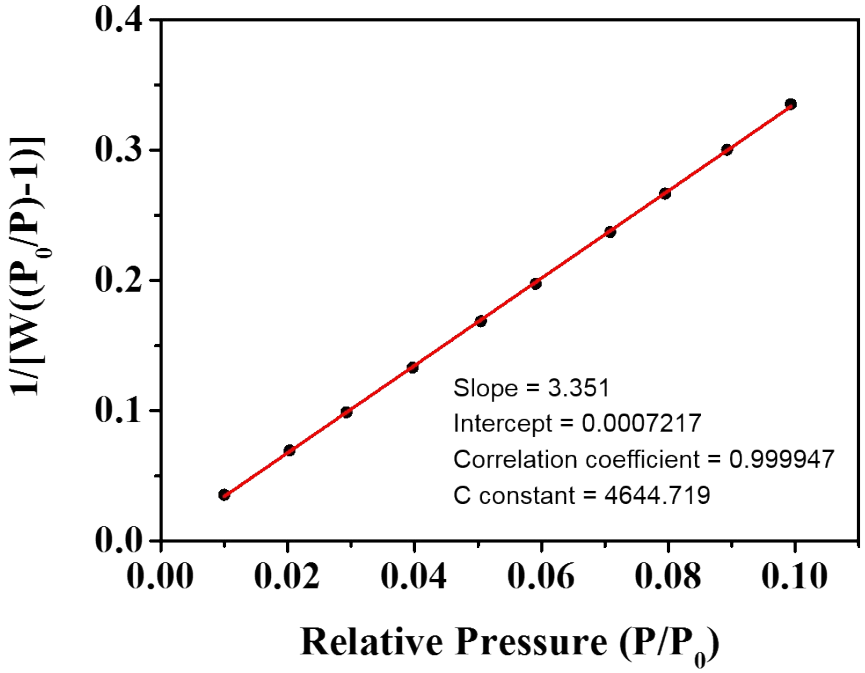

(c)

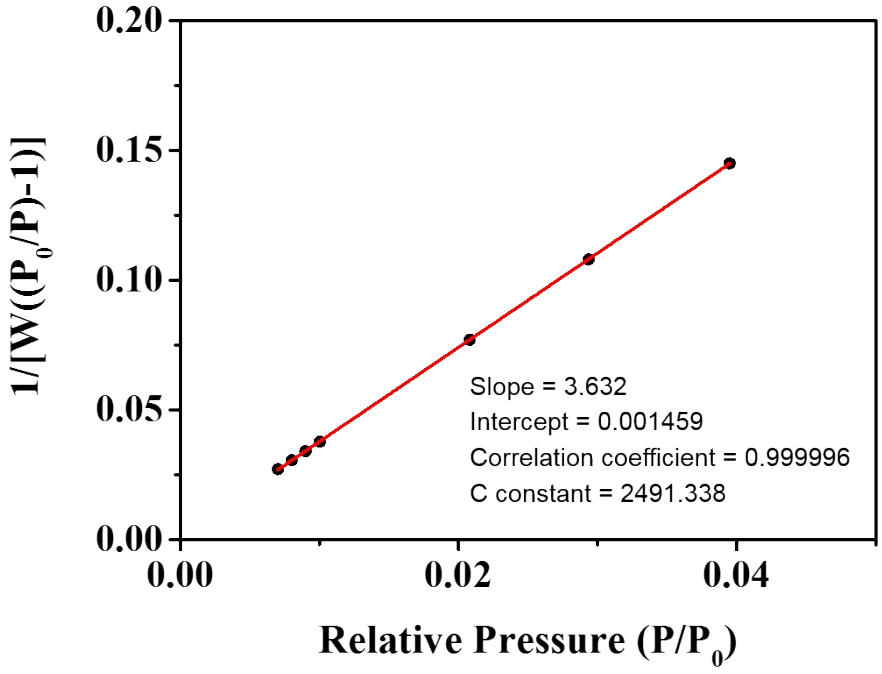

Figure S6. BET plots of (a) M5-1000, (b) M177-1000, (c) B100-1000.

S6. The relation between surface areas of the porous carbons and Zn contents of the parent MOFs

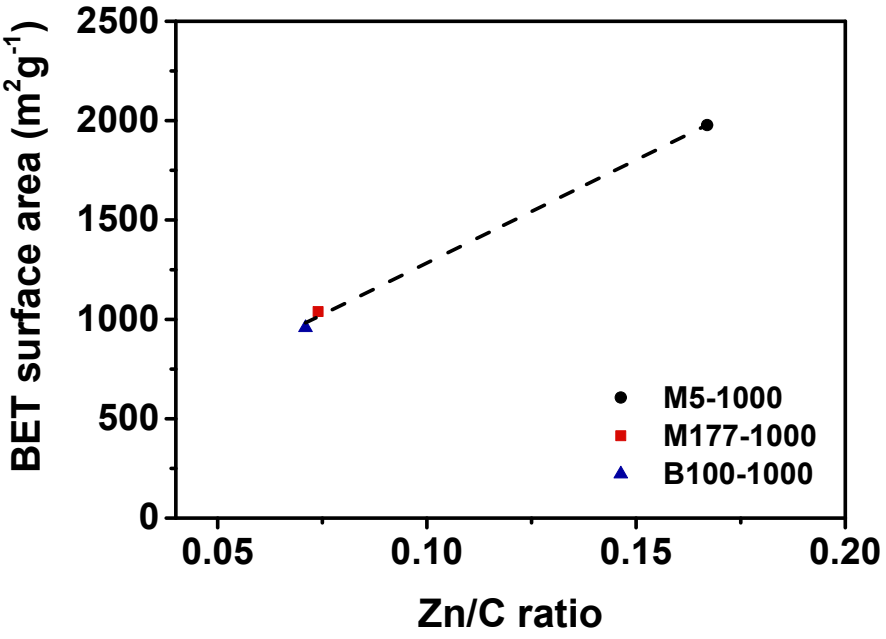

Figure S7. The relation between BET surface areas of the porous carbons and Zn/C ratio of the parent MOFs.

S7. DFT pore size distributions

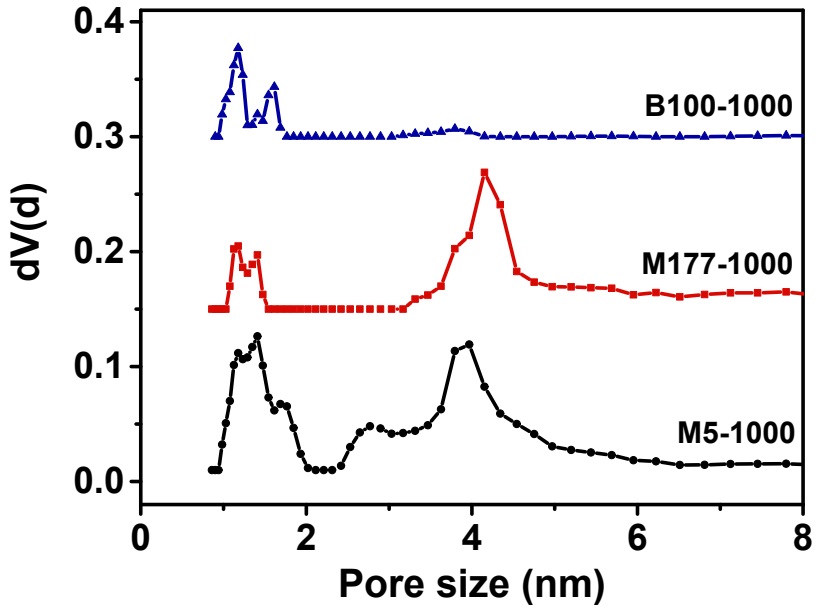

Figure S8. DFT pore size distributions of the porous carbons.

S8. CO_2 adsorption

CO_2 adsorption isotherms at 273 K :

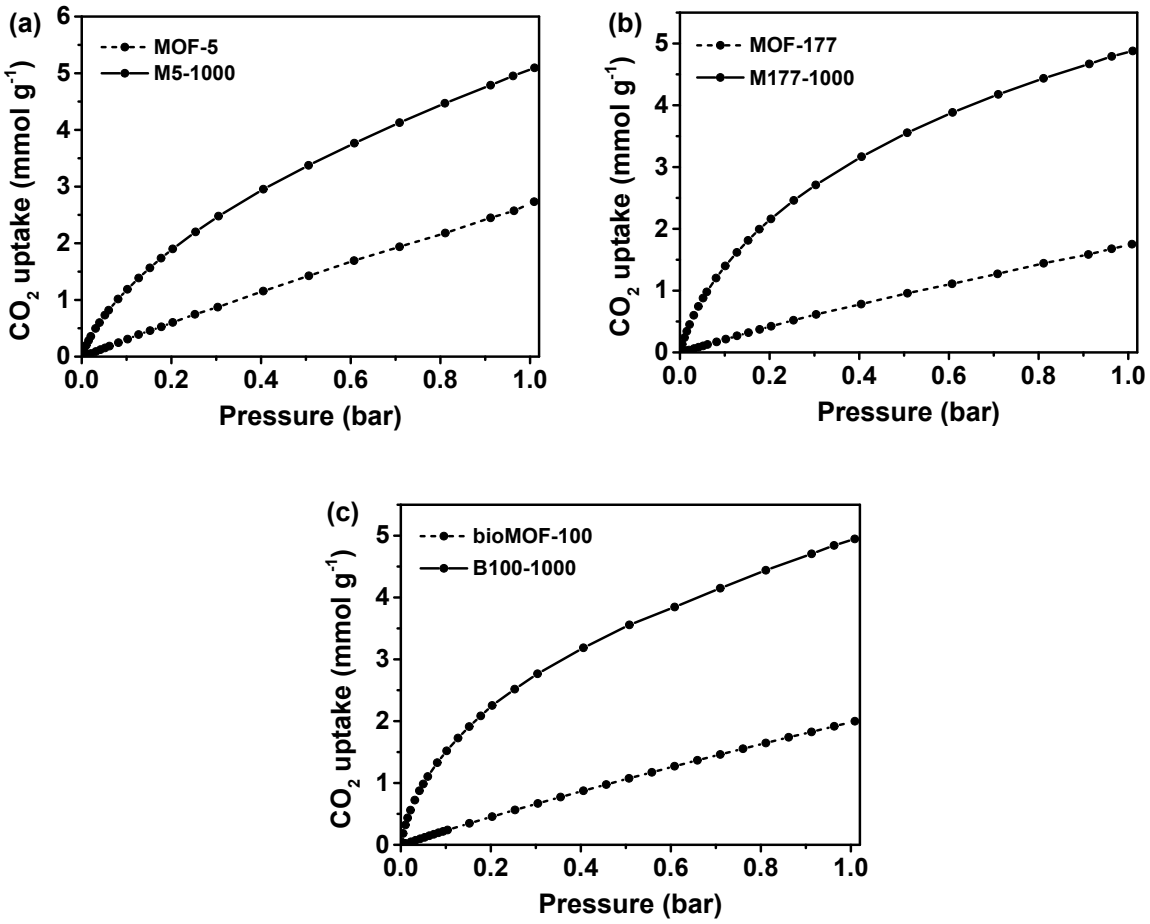

Figure S9. CO_2 adsorption isotherms of pristine MOFs and porous carbons at 273 K.

CO_2 adsorption isotherms at 298 K :

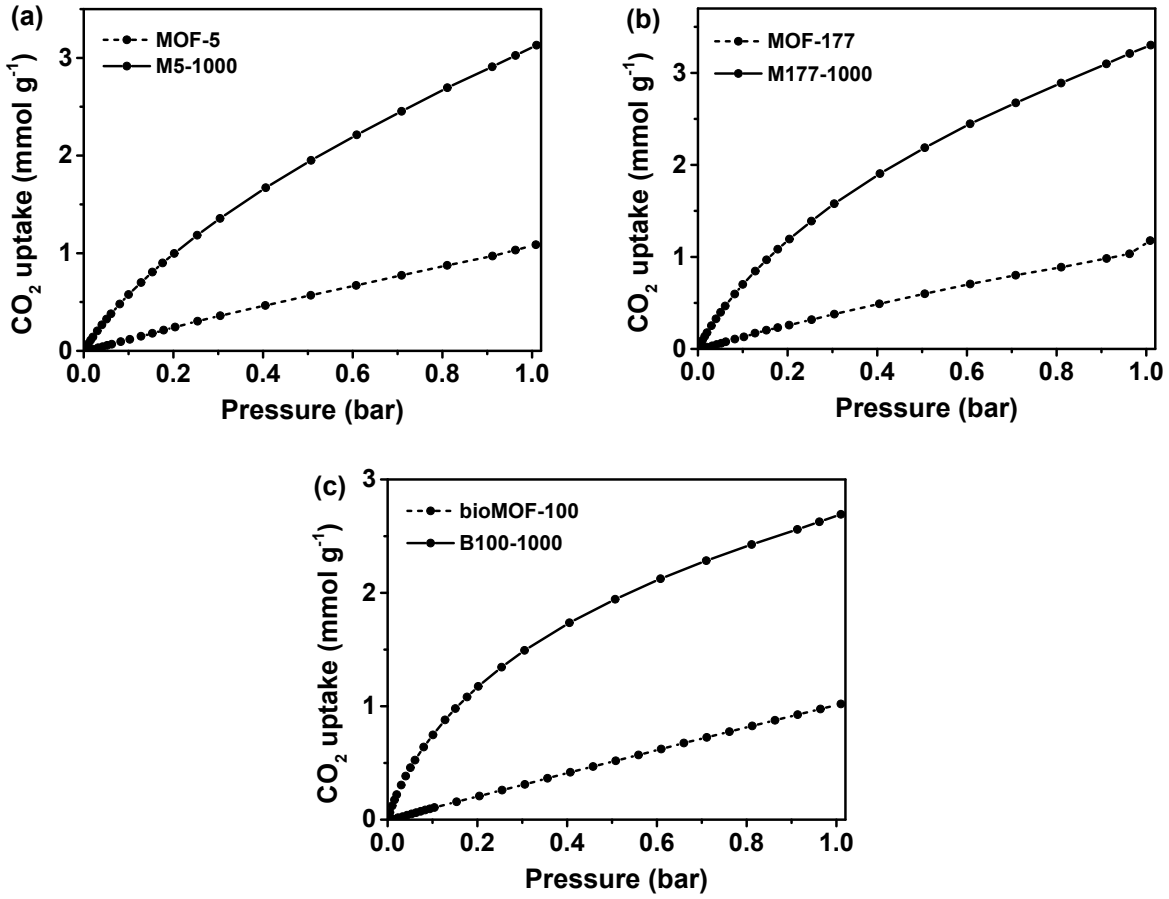

Figure S10. CO_2 adsorption isotherms of pristine MOFs and porous carbons at 298 K.

CO_2 adsorption isotherms at low pressures (273 K) :

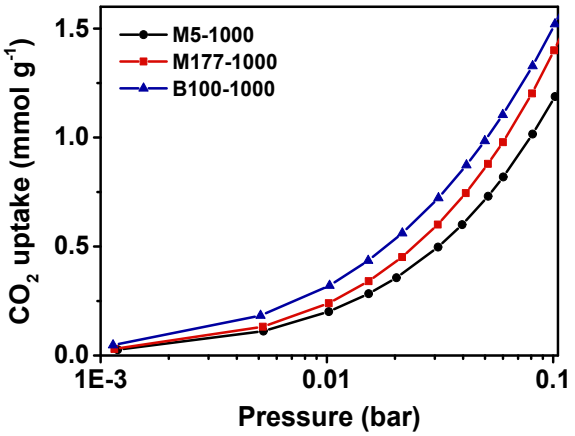

Figure S11. CO_2 adsorption isotherms of the porous carbons at low pressure (273 K).

CO_2 adsorption isotherms at low pressures (298 K) :

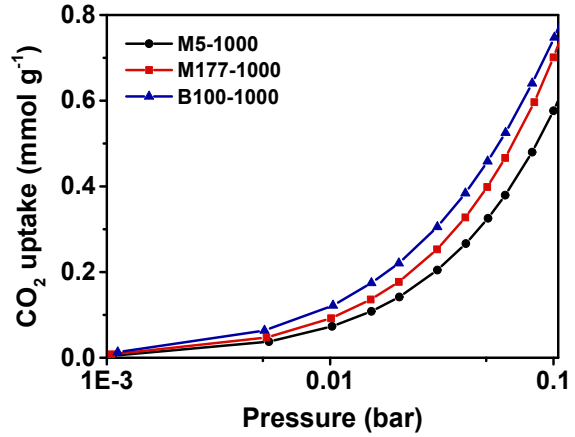

Figure S12. CO_2 adsorption isotherms of the porous carbons at low pressure (298 K).

S9. IAST selectivity

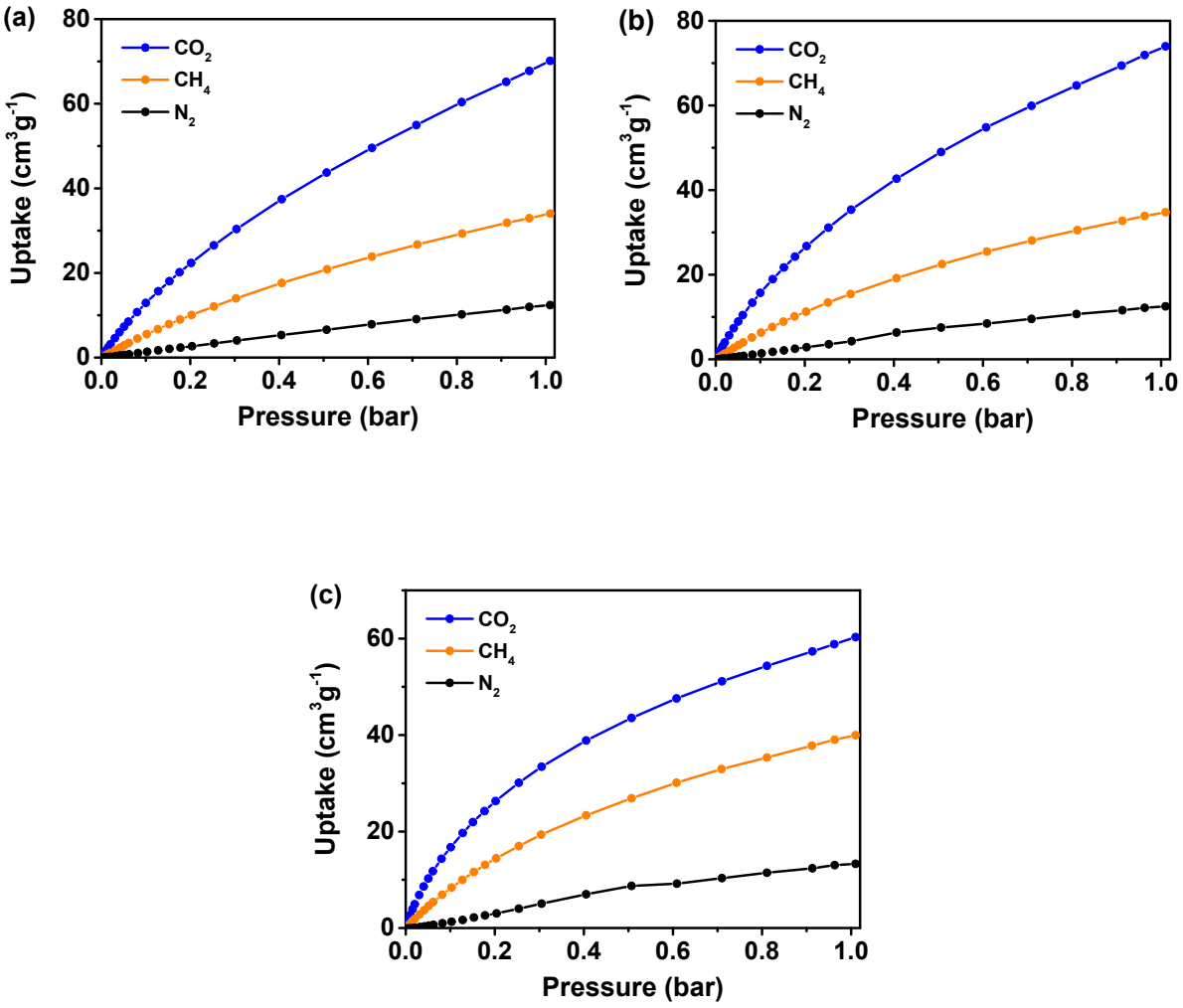

Figure S13. Single-component isotherms of CO_2, CH_4 and N_2 for (a) M5-1000, (b) M177-1000 and (c) B100-1000 at 298 K.

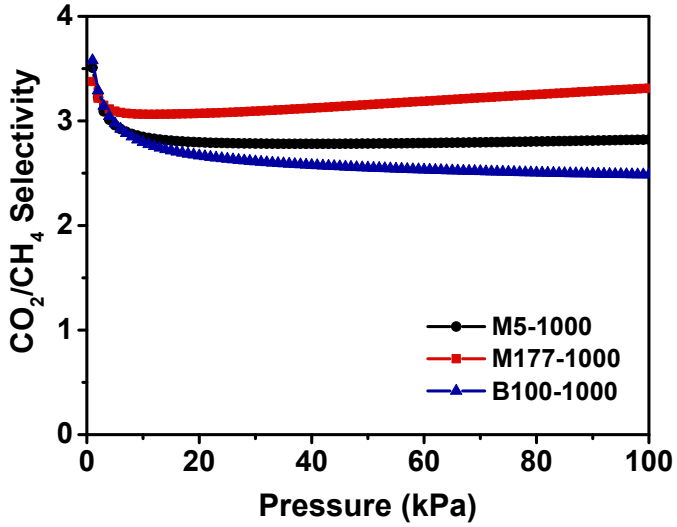

Figure S14. CO_2/CH_4 selectivity of the porous carbons at 298 K.